

Exact solution of the geometrically frustrated spin-1/2 Ising-Heisenberg model on the triangulated Kagomé (triangles-in-triangles) lattice

Jozef Strečka,* Lucia Čanová, and Michal Jaščur

*Department of Theoretical Physics and Astrophysics, Faculty of Science,
P. J. Šafárik University, Park Angelinum 9, 040 01 Košice, Slovak Republic*

Masayuki Hagiwara

*KYOKUGEN (Center for Quantum Science and Technology under Extreme Conditions),
Osaka University, 1-3 Machikaneyama, Toyonaka, Osaka 560-8531, Japan*

(Dated: October 26, 2018)

The geometric frustration of the spin-1/2 Ising-Heisenberg model on the triangulated Kagomé (triangles-in-triangles) lattice is investigated within the framework of an exact analytical method based on the generalized star-triangle mapping transformation. Ground-state and finite-temperature phase diagrams are obtained along with other exact results for the partition function, Helmholtz free energy, internal energy, entropy, and specific heat, by establishing a precise mapping relationship to the corresponding spin-1/2 Ising model on the Kagomé lattice. It is shown that the residual entropy of the disordered spin liquid phase is for the quantum Ising-Heisenberg model significantly lower than for its semi-classical Ising limit ($S_0/N_T k_B = 0.2806$ and 0.4752 , respectively), which implies that quantum fluctuations partially lift a macroscopic degeneracy of the ground-state manifold in the frustrated regime. The investigated model system has an obvious relevance to a series of polymeric coordination compounds $\text{Cu}_9\text{X}_2(\text{cpa})_6$ ($\text{X}=\text{F}, \text{Cl}, \text{Br}$ and $\text{cpa}=\text{carboxypentonic acid}$) for which we made a theoretical prediction about the temperature dependence of zero-field specific heat.

PACS numbers: 05.50.+q, 75.10. Jm, 75.40.Cx, 75.50.Nr

Keywords: Ising-Heisenberg model, triangulated Kagomé lattice, geometric frustration, exact results

I. INTRODUCTION

The antiferromagnetic quantum Heisenberg model (AF-QHM) defined on *geometrically frustrated planar lattices* represents a long-standing theoretical challenge due to a rich variety of unusual ground states it exhibits as a result of the mutual interplay between quantum fluctuations and geometric frustration.^{1,2,3,4} In particular, the extensive theoretical studies of the spin-1/2 AF-QHM on the triangular,⁵ Kagomé,^{6,7} Shastry-Sutherland,⁸ star,⁹ checkerboard,¹⁰ square Kagomé lattice¹¹ and others,¹² have revealed a great diversity in their ground-state and low-temperature behavior. It is now widely accepted that the ground state of the spin-1/2 AF-QHM on some geometrically frustrated planar lattices like a triangular lattice is the Néel-like ordered state,⁵ while there is a still controversial debate whether⁶ or not⁷ the disordered spin liquid state is the true ground state of this model on Kagomé lattice. Anyway, the macroscopic degeneracy of the ground-state manifold turns out to be strongly related to a geometric topology of the underlying lattice and it is therefore of particular research interest to explore a connection between the zero-point entropy and the lattice geometry.

Another striking feature, which currently attracts a great deal of attention to the spin-1/2 AF-QHM on the geometrically frustrated planar lattices, is being a presence of quantized magnetization plateaux in their low-temperature magnetization curves.^{2,3} It is worthwhile to remark that this outstanding quantum phenomenon has already been experimentally observed in several proto-

typical examples of the frustrated quantum spin systems such as the triangular lattice compounds $\text{CsFe}(\text{SO}_4)_2$,¹³ Cs_2CuBr_4 ,¹⁴ and $\text{RbFe}(\text{MoO}_4)_2$,^{13,15} the Kagomé lattice compound $[\text{Cu}_3(\text{titmb})_2(\text{CH}_3\text{COO})_6]\cdot\text{H}_2\text{O}$,¹⁶ and the Shastry-Sutherland lattice compounds $\text{SrCu}_2(\text{BO}_3)_2$ ¹⁷ and RB_4 ($\text{R} = \text{Er}, \text{Tm}$).¹⁸ It also has been demonstrated that the interplay between the geometric frustration and quantum fluctuations might be a driving force for an enhanced magnetocaloric effect emerging during the adiabatic demagnetization.¹⁹ This makes from geometrically frustrated spin systems especially promising refrigerant materials in view of reaching temperatures in a sub-Kelvin range, since they often remain disordered down to the lowest achievable temperatures unlike paramagnetic salts usually exhibiting a spin-glass transition.

The aforementioned scientific achievements have stimulated an intensive search for inorganic molecular materials, whose paramagnetic metal centres connected in the crystal lattice via superexchange pathways would be strongly frustrated by their geometric arrangement.²⁰ From this perspective, the series of isostructural polymeric coordination compounds $\text{Cu}_9\text{X}_2(\text{cpa})_6\cdot n\text{H}_2\text{O}$ ($\text{X}=\text{F}, \text{Cl}, \text{Br}$ and $\text{cpa}=\text{carboxypentonic acid}$)²¹ belongs to the most fascinating geometrically frustrated materials on behalf of a beautiful architecture of their magnetic lattice. The magnetic lattice of this series is built up of divalent copper (Cu^{2+}) ions situated at two crystallographically inequivalent lattice positions (see Fig. 1). Cu^{2+} ions with a square pyramidal coordination (a -sites) form equilateral triangles (trimers), which are inter-connected to one another by Cu^{2+} ions (monomers) with an elon-

gated octahedral coordination (b -sites). The lattice positions of the b -sites constitute the regular Kagomé network, whereas each monomeric b -site is connected via four bonds to two adjacent trimers of the a -sites. This magnetic architecture can be accordingly regarded as the triangulated Kagomé (triangles-in-triangles) lattice, since smaller triangles of the trimeric a -sites are in fact embedded in larger triangles of the monomeric b -sites forming the basic Kagomé pattern.

Experimental studies reported on this family of compounds reveal obvious manifestations of the geometric frustration. All three isomorphous compounds do not order down to 1.7 K,²² the magnetization shows a plateau around one third of the saturation magnetization and it does not saturate up to 38 T.²³ Furthermore, the temperature dependence of inverse susceptibility indicates two temperature regimes inherent to two different exchange pathways. The linear dependence of the inverse susceptibility is well fitted by the Curie-Weiss law within the temperature interval between 150–250 K with the respective Weiss constants $\Theta_w = -237$ K, -226 K, and -243 K for the fluoro, chloro, and bromo analogue²², respectively, while the Weiss constant of the best Curie-Weiss fit generally increases up to roughly $\Theta_w = 6$ K in the temperature range below 50 K.²³ These observations would suggest an extremely high frustration ratio $f = |\Theta_w|/T_c > 130$ (T_c is the ordering temperature)²⁴ for each member of the $\text{Cu}_9\text{X}_2(\text{cpa})_6$ family, which makes from this series a prominent class of the highly frustrated materials that possibly display the spin liquid ground state. Based on the considerations of exchange pathways, the strong antiferromagnetic interaction has been assigned to the exchange interaction J_{aa} between the trimeric a -sites, while the weaker (possibly ferromagnetic) interaction has been ascribed to the exchange interaction J_{ab} between the trimeric a -sites and the monomeric b -sites. The overall ratio between both exchange constants might be estimated from the corresponding ratio between the Weiss constants extrapolated from the high- and low-temperature regime yielding $|J_{aa}/J_{ab}| \approx 40$.

Motivated by these experiments, Zheng and Sun²⁵ have calculated an exact phase diagram of the spin-1/2 Ising model on the triangulated Kagomé lattice and the validity of this phase diagram has recently been confirmed by an independent exact calculation of Loh, Yao, and Carlson.²⁶ In addition to the exact ground-state and finite-temperature phase diagrams, the authors of the latter work also presented exact analytical results for several thermodynamic quantities (partition function, Helmholtz free energy, internal energy, entropy, and specific heat), which were complemented by the Monte Carlo simulations corroborating these exact analytical results and bringing other accurate numerical results for the magnetization and susceptibility in the zero as well as non-zero magnetic field.²⁶ Among the most interesting findings being reported is certainly a theoretical prediction of the spin liquid phase with a large residual entropy per spin $S_0/N_T k_B = \frac{1}{9} \ln 72 = 0.4752$, which appears in the

ground state on assumption of a sufficiently strong antiferromagnetic intra-trimer interaction $J_{aa}/|J_{ab}| < -1$ (see for details Section IV.A in Ref. 26).

Unfortunately, the theoretical description based on the Ising model might fail in describing many important vestiges of the most of copper-based coordination compounds, since they usually exhibit a rather isotropic magnetic behavior.²⁷ Beside this, the Ising model description completely disregards the effect of quantum fluctuations, which might play a crucial role in determining the magnetic behavior of coordination compounds incorporating paramagnetic Cu^{2+} ions having the lowest possible quantum spin number $S = 1/2$. Therefore, the spin-1/2 quantum Heisenberg model is usually thought of as being much more appropriate model for the copper-based coordination compounds.²⁷ In accordance with this statement, ESR measurements performed on the $\text{Cu}_9\text{X}_2(\text{cpa})_6$ series have shown just a minor anisotropy in the g -factor that also serves in evidence of a negligible magnetic anisotropy.^{23,28}

Of course, the spin-1/2 quantum Heisenberg model is very difficult to deal with due to insurmountable mathematical complexities associated with a non-commutability between spin operators involved in its Hamiltonian and thus, one has usually to rely either on applicability of some simpler approximative method or to perform rather extensive numerical calculations. To the best of our knowledge, the spin-1/2 Heisenberg model on the triangulated Kagomé lattice has been studied yet merely in terms of the linear Holstein-Primakoff spin wave theory²⁹ and the variational mean-field like treatment.³⁰ Both the aforementioned methods have however obvious insufficiencies. The former method based on the spin-wave approximation is applicable only if the ratio between both interaction parameters is from the interval $1 \leq |J_{aa}/J_{ab}| \leq 3$, i.e. the frustrating antiferromagnetic intra-trimer interaction J_{aa} might not be much too stronger than the ferromagnetic one J_{ab} . On the other hand, the latter method based on the variational mean-field like treatment is asymptotically exact in the $|J_{ab}/J_{aa}| \rightarrow 0$ limit, but it even fails to predict the disordered ground state for any finite ratio $|J_{ab}/J_{aa}|$.²⁶

In view of this, the present work aims to suggest and exactly solve the spin-1/2 Ising-Heisenberg model on the triangulated Kagomé lattice by establishing a precise mapping relationship with the corresponding spin-1/2 Ising model on the simple Kagomé lattice. Within the framework of the proposed Ising-Heisenberg model, the exchange interaction between the trimeric a -sites is being treated as the XXZ Heisenberg interaction $J_{aa} = J_H(\Delta)$, while the exchange interaction between the trimeric a -sites and monomeric b -sites will be approximated by the Ising-type interaction $J_{ab} = J_I$. Even although this model also has a clear deficiency in that the monomer-trimer interaction is being considered as the Ising-type interaction, it should be much more reliable in describing a frustrated magnetism of $\text{Cu}_9\text{X}_2(\text{cpa})_6$ compounds as it correctly takes into account quantum fluctuations

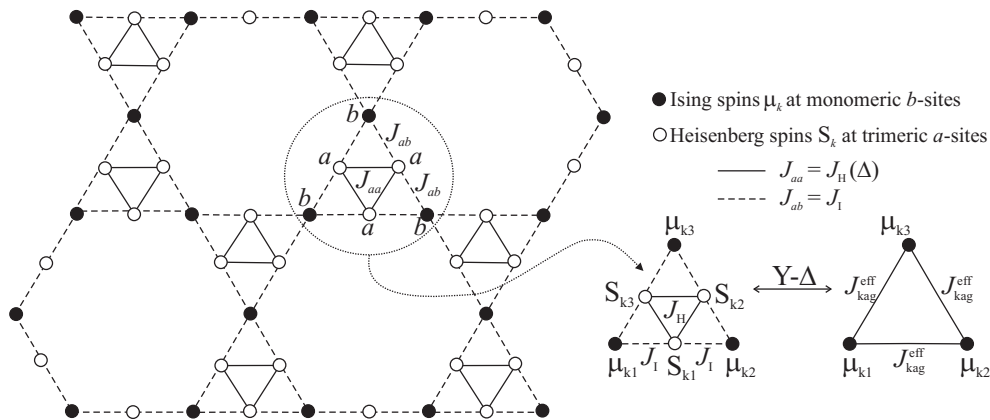


FIG. 1: The cross-section of the triangulated Kagomé (triangles-in-triangles) lattice. The empty and full circles denote lattice positions of the trimeric a -sites and monomeric b -sites, respectively, which are occupied within the proposed Ising-Heisenberg model by the Heisenberg and Ising spins. Solid and broken lines schematically reproduce the intra-trimer Heisenberg interaction $J_{aa} = J_H(\Delta)$ and the monomer-trimer Ising interaction $J_{ab} = J_I$. The ellipse demarcates a six-spin cluster described by the Hamiltonian (2), which can be mapped by the use of generalized star-triangle transformation into a simple triangle of the Ising spins mutually interacting via the effective exchange coupling βJ_{kag}^{eff} .

between the trimeric a -sites. In addition, it is also quite plausible to argue that the monomeric b -sites are in the frustrated regime completely free to flip without any energy cost and hence, the Ising character of the monomer-trimer interaction might be regarded as at least quite reasonable first-order approximation.

The rest of this paper is organized as follows. In Section II, we will provide a detailed description of the model under investigation and then, basic steps of our exact analytical treatment will be explained. The most interesting results are presented and detailed discussed in Section III, where a particular emphasis is laid on a physical understanding of the ground-state and finite-temperature phase diagrams, as well as, the temperature dependences of several thermodynamical quantities. Some conclusions are finally drawn in Section IV.

II. MODEL AND ITS EXACT SOLUTION

Let us define the spin-1/2 Ising-Heisenberg model on the triangulated Kagomé lattice (Fig. 1), which resembles a rather curious magnetic structure discovered in the series of polymeric coordination compounds $Cu_9X_2(cpa)_6$.²¹ The magnetic properties of this series are captured to the lattice positions of Cu^{2+} ions, which are situated at two inequivalent lattice positions previously referred to as the trimeric a -sites (empty circles) and the monomeric b -sites (full circles), respectively. Let us now assign the *Heisenberg spin* $S = 1/2$ to each trimeric a -site

and the *Ising spin* $\mu = 1/2$ to each monomeric b -site.³⁸ In this way, the exchange interaction J_{aa} between Cu^{2+} ions located at the nearest-neighbor trimeric sites will be treated as the Heisenberg interaction $J_H(\Delta)$, while the exchange interaction J_{ab} between two Cu^{2+} ions located at the nearest-neighbor trimeric and monomeric sites will be treated as the Ising interaction J_I . The total Hamiltonian of the model under investigation then reads

$$\hat{\mathcal{H}} = -J_H \sum_{(i,j)} \left[\Delta (\hat{S}_i^x \hat{S}_j^x + \hat{S}_i^y \hat{S}_j^y) + \hat{S}_i^z \hat{S}_j^z \right] - J_I \sum_{(k,l)} \hat{S}_k^z \hat{\mu}_l^z, \quad (1)$$

where the first summation is carried out over all pairs of the nearest-neighbor Heisenberg spins and the second summation extends over all pairs of the nearest-neighbor Heisenberg and Ising spins, respectively. The spin operators \hat{S}_i^α ($\alpha = x, y, z$) and $\hat{\mu}_i^z$ denote spatial components the usual spin-1/2 operator and the parameter Δ will allow us to control the exchange anisotropy in the anisotropic XXZ Heisenberg interaction and to obtain the Ising model as a special limiting case for $\Delta = 0$. Finally, the total number of the Ising spins (b -sites) is set to N , which implies that the total number of all spins (lattice sites) is $N_T = 3N$.

For further convenience, the total Hamiltonian (1) can be written as a sum over six-spin cluster Hamiltonians $\hat{\mathcal{H}} = \sum_k \hat{\mathcal{H}}_k$, whereas each cluster Hamiltonian $\hat{\mathcal{H}}_k$ involves all the interaction terms associated with three Heisenberg spins from k th trimer (see Fig. 1)

$$\begin{aligned} \hat{\mathcal{H}}_k = & - J_H \left[\Delta (\hat{S}_{k1}^x \hat{S}_{k2}^x + \hat{S}_{k1}^y \hat{S}_{k2}^y) + \hat{S}_{k1}^z \hat{S}_{k2}^z \right] - J_H \left[\Delta (\hat{S}_{k2}^x \hat{S}_{k3}^x + \hat{S}_{k2}^y \hat{S}_{k3}^y) + \hat{S}_{k2}^z \hat{S}_{k3}^z \right] \\ & - J_H \left[\Delta (\hat{S}_{k3}^x \hat{S}_{k1}^x + \hat{S}_{k3}^y \hat{S}_{k1}^y) + \hat{S}_{k3}^z \hat{S}_{k1}^z \right] - \hat{S}_{k1}^z (h_{k1} + h_{k2}) - \hat{S}_{k2}^z (h_{k2} + h_{k3}) - \hat{S}_{k3}^z (h_{k3} + h_{k1}), \end{aligned} \quad (2)$$

where $h_{ki} = J_I \hat{\mu}_{ki}^z$. Obviously, the six-spin cluster Hamiltonian (2) might be regarded as the Hamiltonian of k th Heisenberg trimer placed in some generally non-uniform magnetic field produced by three surrounding Ising spins. By taking into account the commutability between different cluster Hamiltonians $[\hat{\mathcal{H}}_i, \hat{\mathcal{H}}_j] = 0$ valid for each $i \neq j$, the partition function of the spin-1/2 Ising-Heisenberg model on the triangulated Kagomé lattice can be partially factorized into the product of cluster partition functions \mathcal{Z}_k

$$\mathcal{Z} = \sum_{\{\mu_i\}} \prod_{k=1}^{2N/3} \text{Tr}_k \exp(-\beta \hat{\mathcal{H}}_k) = \sum_{\{\mu_i\}} \prod_{k=1}^{2N/3} \mathcal{Z}_k. \quad (3)$$

Above, the summation $\sum_{\{\mu_i\}}$ runs over all possible spin

configurations of the Ising spins and the symbol Tr_k stands for a trace over spin degrees of freedom of k th Heisenberg trimer. To proceed further with the calculation, it is very convenient to accomplish an exact analytical diagonalization of the cluster Hamiltonian (2) in a particular Hilbert subspace corresponding to k th Heisenberg trimer. If doing so, the resulting cluster partition function \mathcal{Z}_k will depend just upon three Ising spins μ_{k1} , μ_{k2} , and μ_{k3} , which are included in the parameters h_{k1} , h_{k2} , and h_{k3} determining the 'local magnetic fields' acting on the Heisenberg spins. Moreover, the explicit mathematical form of the cluster partition function \mathcal{Z}_k immediately implies a possibility of performing the generalized star-triangle mapping transformation^{31,32}

$$\begin{aligned} \mathcal{Z}_k &= 2 \exp\left(\frac{3\beta J_H}{4}\right) \cosh[\beta J_I(\mu_{k1}^z + \mu_{k2}^z + \mu_{k3}^z)] \\ &+ \exp\left[-\frac{\beta J_H}{4} + \frac{\beta J_I}{3}(\mu_{k1}^z + \mu_{k2}^z + \mu_{k3}^z)\right] \sum_{n=0}^2 \exp\left[-2\beta \text{sgn}(Q_+) \sqrt{P} \cos\left(\Phi_+ + \frac{2\pi n}{3}\right)\right] \\ &+ \exp\left[-\frac{\beta J_H}{4} - \frac{\beta J_I}{3}(\mu_{k1}^z + \mu_{k2}^z + \mu_{k3}^z)\right] \sum_{n=0}^2 \exp\left[-2\beta \text{sgn}(Q_-) \sqrt{P} \cos\left(\Phi_- + \frac{2\pi n}{3}\right)\right] \\ &= A \exp\left[\beta J_{\text{kag}}^{\text{eff}} (\mu_{k1}^z \mu_{k2}^z + \mu_{k2}^z \mu_{k3}^z + \mu_{k3}^z \mu_{k1}^z)\right], \end{aligned} \quad (4)$$

where $\beta = 1/(k_B T)$, k_B is Boltzmann's constant, T the absolute temperature, and the parameters P , Q_{\pm} , and Φ_{\pm} are defined as follows

$$P = \left(\frac{J_I}{3}\right)^2 \left[\frac{3}{4} - (\mu_{k1}^z \mu_{k2}^z + \mu_{k2}^z \mu_{k3}^z + \mu_{k3}^z \mu_{k1}^z)\right] + \left(\frac{J_H \Delta}{2}\right)^2, \quad (5)$$

$$Q_{\pm} = \pm \frac{1}{2} \left(\frac{J_I}{3}\right)^3 [\mu_{k1}^z + \mu_{k2}^z + \mu_{k3}^z - 12\mu_{k1}^z \mu_{k2}^z \mu_{k3}^z] - \left(\frac{J_H \Delta}{2}\right)^3, \quad (6)$$

$$\Phi_{\pm} = \frac{1}{3} \arctan\left(\frac{\sqrt{P^3 - Q_{\pm}^2}}{Q_{\pm}}\right). \quad (7)$$

From here onward, our procedure closely follows the approach developed by Zheng and Sun that relates an ex-

act solution of the spin-1/2 Ising model on the triangulated Kagomé lattice to an exact solution of the the corresponding spin-1/2 Ising model on the simple Kagomé lattice.²⁵ As a matter of fact, the star-triangle transformation (4) effectively removes all the interaction terms associated with k th Heisenberg trimer and substitutes them by the effective interaction $J_{\text{kag}}^{\text{eff}}$ between three enclosing Ising spins μ_{k1} , μ_{k2} , and μ_{k3} . Of course, the mapping transformation (4) must hold for any available spin configuration of three enclosing Ising spins and this self-consistency condition unambiguously determines so far not specified mapping parameters A and $\beta J_{\text{kag}}^{\text{eff}}$

$$A = (V_1 V_2^3)^{1/4} \quad \text{and} \quad \beta J_{\text{kag}}^{\text{eff}} = \ln(V_1/V_2). \quad (8)$$

The functions V_1 and V_2 entering into the effective mapping parameters A and $\beta J_{\text{kag}}^{\text{eff}}$ are actually two independent expressions for the cluster partition function (4) to be obtained by considering all eight possible spin configurations available to three enclosing Ising spins

$$V_1 = 2 \exp\left(\frac{3\beta J_H}{4}\right) \cosh\left(\frac{3\beta J_I}{2}\right) + 2 \exp\left(-\frac{\beta J_H}{4}\right) \cosh\left(\frac{\beta J_I}{2}\right) \left[\exp(\beta J_H \Delta) + 2 \exp\left(-\frac{\beta J_H \Delta}{2}\right) \right], \quad (9)$$

$$V_2 = 2 \exp\left(\frac{3\beta J_H}{4}\right) \cosh\left(\frac{\beta J_I}{2}\right) + \exp\left(-\frac{\beta J_H}{4} + \frac{\beta J_I}{6}\right) \sum_{n=0}^2 \exp\left[-2\beta \text{sgn}(q_+) \sqrt{p} \cos\left(\phi_+ + \frac{2\pi n}{3}\right)\right] \\ + \exp\left(-\frac{\beta J_H}{4} - \frac{\beta J_I}{6}\right) \sum_{n=0}^2 \exp\left[-2\beta \text{sgn}(q_-) \sqrt{p} \cos\left(\phi_- + \frac{2\pi n}{3}\right)\right], \quad (10)$$

and the parameters p , q_{\pm} , and ϕ_{\pm} are defined as follows

$$p = \left(\frac{J_I}{3}\right)^2 + \left(\frac{J_H \Delta}{2}\right)^2, \quad (11)$$

$$q_{\pm} = \pm \left(\frac{J_I}{3}\right)^3 - \left(\frac{J_H \Delta}{2}\right)^3, \quad (12)$$

$$\phi_{\pm} = \frac{1}{3} \arctan\left(\frac{\sqrt{p^3 - q_{\pm}^2}}{q_{\pm}}\right). \quad (13)$$

By substituting the mapping transformation (4) into the relevant expression for the partition function (3) one establishes a simple mapping relationship between the partition function of the spin-1/2 Ising-Heisenberg model on the triangulated Kagomé lattice and the partition function of the corresponding spin-1/2 Ising model on the Kagomé lattice

$$\mathcal{Z}(\beta, J_H, \Delta, J_I) = A^{2N/3} \mathcal{Z}_{\text{kag}}(\beta J_{\text{kag}}^{\text{eff}}). \quad (14)$$

This relation actually completes our exact calculation of the partition function as the corresponding exact result for the partition function of the spin-1/2 Ising model on the Kagomé lattice is well known.^{33,34,35} At this stage, exact results for other thermodynamic quantities follow

straightforwardly. The Helmholtz free energy of the spin-1/2 Ising-Heisenberg model on the triangulated Kagomé lattice may be connected to the Helmholtz free energy of the corresponding spin-1/2 Ising model on the Kagomé lattice ($\mathcal{F}_{\text{kag}} = -\beta^{-1} \ln \mathcal{Z}_{\text{kag}}$) through the relation

$$\mathcal{F} = \mathcal{F}_{\text{kag}} - 2N\beta^{-1} \ln A/3. \quad (15)$$

The connection between the internal energy of spin-1/2 Ising-Heisenberg model on the triangulated Kagomé lattice and that of the corresponding spin-1/2 Ising model on the Kagomé lattice can readily be obtained by differentiating the logarithm of Eq. (14) with respect to the inverse temperature β yielding

$$\mathcal{U} = -\frac{\partial \ln \mathcal{Z}}{\partial \beta} = -\frac{2N}{3} \frac{\partial \ln A}{\partial \beta} - \frac{\partial \ln \mathcal{Z}_{\text{kag}}}{\partial(\beta J_{\text{kag}}^{\text{eff}})} \frac{\partial(\beta J_{\text{kag}}^{\text{eff}})}{\partial \beta} \\ = \frac{W_1}{V_1} \left(\frac{\mathcal{U}_{\text{kag}}}{J_{\text{kag}}^{\text{eff}}} - \frac{N}{6} \right) - \frac{W_2}{V_2} \left(\frac{\mathcal{U}_{\text{kag}}}{J_{\text{kag}}^{\text{eff}}} + \frac{N}{2} \right). \quad (16)$$

Note that the exact result for the internal energy of the spin-1/2 Ising model on the Kagomé lattice is well known (see for instance Ref. 35) and thus, our exact calculation is essentially completed by introducing the parameters W_1 and W_2 that denote inverse temperature derivatives of the functions V_1 and V_2 given by Eqs. (9) and (10)

$$W_1 = \frac{\partial V_1}{\partial \beta} = \frac{3}{2} \exp\left(\frac{3\beta J_H}{4}\right) \left[J_H \cosh\left(\frac{3\beta J_I}{2}\right) + 2J_I \sinh\left(\frac{3\beta J_I}{2}\right) \right] \\ + \exp\left(-\frac{\beta J_H}{4} + \beta J_H \Delta\right) \left[\left(2J_H \Delta - \frac{J_H}{2}\right) \cosh\left(\frac{\beta J_I}{2}\right) + J_I \sinh\left(\frac{\beta J_I}{2}\right) \right] \\ - \exp\left(-\frac{\beta J_H}{4} - \frac{\beta J_H \Delta}{2}\right) \left[\left(2J_H \Delta + J_H\right) \cosh\left(\frac{\beta J_I}{2}\right) - 2J_I \sinh\left(\frac{\beta J_I}{2}\right) \right], \quad (17)$$

$$W_2 = \frac{\partial V_2}{\partial \beta} = \exp\left(\frac{3\beta J_H}{4}\right) \left[\frac{3}{2} J_H \cosh\left(\frac{\beta J_I}{2}\right) + J_I \sinh\left(\frac{\beta J_I}{2}\right) \right] \\ - \sum_{n=0}^2 \left[\frac{J_H}{4} - \frac{J_I}{6} + 2\text{sgn}(q_+) \sqrt{p} \cos\left(\phi_+ + \frac{2\pi n}{3}\right) \right] \exp\left[-\frac{\beta J_H}{4} + \frac{\beta J_I}{6} - 2\beta \text{sgn}(q_+) \sqrt{p} \cos\left(\phi_+ + \frac{2\pi n}{3}\right)\right] \\ - \sum_{n=0}^2 \left[\frac{J_H}{4} + \frac{J_I}{6} + 2\text{sgn}(q_-) \sqrt{p} \cos\left(\phi_- + \frac{2\pi n}{3}\right) \right] \exp\left[-\frac{\beta J_H}{4} - \frac{\beta J_I}{6} - 2\beta \text{sgn}(q_-) \sqrt{p} \cos\left(\phi_- + \frac{2\pi n}{3}\right)\right]. \quad (18)$$

The entropy can be now easily calculated either from the basic thermodynamic relation between Helmholtz free energy and internal energy $\mathcal{F} = \mathcal{U} - T\mathcal{S}$, or as a negative temperature derivative of the free energy (15). Both procedures yield the following closed-form relation for the reduced entropy per one site of the original spin-1/2 Ising-Heisenberg model on the triangulated Kagomé lattice

$$\frac{\mathcal{S}}{N_{\text{T}}k_{\text{B}}} = \frac{1}{3N} \ln \mathcal{Z}_{\text{kag}} + \frac{2}{9} \ln A + \frac{\beta W_1}{3V_1} \left(\frac{\mathcal{U}_{\text{kag}}}{N J_{\text{kag}}^{\text{eff}}} - \frac{1}{6} \right) - \frac{\beta W_2}{3V_2} \left(\frac{\mathcal{U}_{\text{kag}}}{N J_{\text{kag}}^{\text{eff}}} + \frac{1}{2} \right). \quad (19)$$

It is quite obvious from the above formula that the reduced entropy of the spin-1/2 Ising-Heisenberg model on the triangulated Kagomé lattice can be expressed in terms of the known exact results for the partition function³⁴ and internal energy³⁵ of the corresponding spin-1/2 Ising model on the Kagomé lattice. It is worthy to note, moreover, that the zero-field specific heat can also be simply obtained as a temperature derivative of the internal energy (16), but the final expression is too cumbersome to write it down here explicitly.

III. RESULTS AND DISCUSSION

Before proceeding to a discussion of the most interesting results, it is quite useful to realize that all final results derived in the foregoing section are invariant under the transformation $J_{\text{I}} \rightarrow -J_{\text{I}}$. For this reason, it is very convenient to set the absolute value of the Ising interaction $|J_{\text{I}}|$ as the energy unit and to define two dimensionless parameters $k_{\text{B}}T/|J_{\text{I}}|$ and $J_{\text{H}}/|J_{\text{I}}|$ reducing the number of free parameters. The former dimensionless parameter is then proportional to a relative size of the temperature, while the latter one determines a relative strength of the intra-trimer Heisenberg interaction J_{H} with respect to the monomer-trimer Ising interaction J_{I} .

First, let us take a closer look at the ground-state behavior. It is quite evident that the spin-1/2 Ising-Heisenberg model on the triangulated Kagomé lattice exhibits spontaneous long-range ordering if and only if the corresponding spin-1/2 Ising model on the simple Kagomé lattice is spontaneously long-range ordered as well. Accordingly, the ground-state phase diagram can readily be obtained from a comparison of the effective interaction parameter $\beta J_{\text{kag}}^{\text{eff}}$ given by Eq. (8) with the critical point of the spin-1/2 Ising model on the Kagomé lattice $\beta_{\text{c}} J_{\text{kag}} = \ln(3 + 2\sqrt{3})$ [$\beta_{\text{c}} = 1/(k_{\text{B}}T_{\text{c}})$, T_{c} is the critical temperature].³³ In the consequence of that, the ground state is spontaneously long-range ordered if $\beta J_{\text{kag}}^{\text{eff}} > \ln(3 + 2\sqrt{3})$, while it becomes disordered spin liquid state as long as $\beta J_{\text{kag}}^{\text{eff}} < \ln(3 + 2\sqrt{3})$. The phase boundary between ordered and disordered ground states, which follows from the zero-temperature limit of the

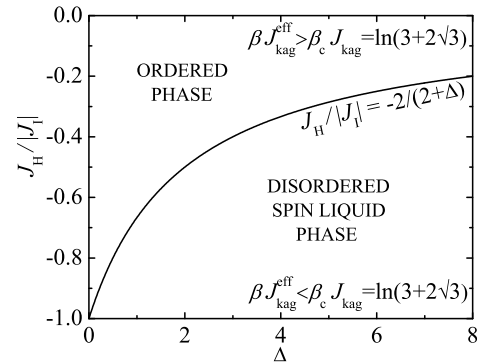


FIG. 2: Ground-state phase diagram in the $\Delta - J_{\text{H}}/|J_{\text{I}}|$ plane separating the spontaneously ordered and disordered phases.

mapping parameter (8), is shown in Fig. 2 and can be expressed through the following analytical condition

$$J_{\text{H}}/|J_{\text{I}}| = -2/(2 + \Delta). \quad (20)$$

It can be easily understood that the disordered spin liquid state appears as a result of geometric frustration, which comes into play provided that there is a sufficiently strong antiferromagnetic Heisenberg interaction. Indeed, the ground state is a simple ferromagnetic or ferrimagnetic spin arrangement for any $J_{\text{H}}/|J_{\text{I}}|$ greater than the boundary value (20) depending on whether $J_{\text{I}} > 0$ or $J_{\text{I}} < 0$, otherwise it becomes the disordered spin liquid state. Apparently, the greater is the anisotropy constant Δ , the weaker antiferromagnetic Heisenberg interaction is needed to destroy the spontaneous long-range ordering.

Now, let us make few remarks on a nature of possible ground states. The ferromagnetic as well as ferrimagnetic ordered states can be characterized through the same classical spin ordering as previously described by the analysis of the spin-1/2 Ising model on the triangulated Kagomé lattice.²⁶ As far as the disordered spin liquid state is concerned, however, there is a fundamental difference between the disordered ground state of the spin-1/2 Ising-Heisenberg model with any $\Delta \neq 0$ and its semi-classical Ising limit $\Delta = 0$, respectively. As a matter of fact, considering the frustrated regime $J_{\text{H}}/|J_{\text{I}}| < -1$ and setting $\Delta = 0$ into Eq. (8) gives the zero effective exchange coupling $\beta J_{\text{kag}}^{\text{eff}} = 0$, which means that the disordered ground state of the spin-1/2 Ising model on the triangulated Kagomé lattice is equivalent to an ensemble of non-interacting spins, or equivalently, to a spin system at infinite temperature. This implies that the Ising spins at the monomeric b -sites are completely free to flip and the ground-state degeneracy of the disordered spin liquid state can be straightforwardly counted by following the argumentation of Loh, Yao, and Carlson.²⁶ The residual entropy per spin is accordingly $S_0/N_{\text{T}}k_{\text{B}} = \frac{1}{9} \ln 72 = 0.4752$, since each trimeric unit has precisely three different lowest-energy states for each possible spin configuration of its three surrounding monomeric spins and the basic unit cell contains two

trimeric units and three monomeric spins.

Contrary to this, the effective exchange coupling (8) that corresponds to the spin-1/2 Ising-Heisenberg model on the triangulated Kagomé lattice with any $\Delta \neq 0$ is equal to $\beta J_{\text{kag}}^{\text{eff}} = \ln 2$ in the disordered region. Even although this value is smaller than the critical value $\beta_c J_{\text{kag}}$ and the spin system must be consequently disordered, its positive and non-zero value indicates a ferromagnetic character of short-range correlations between the monomeric Ising spins. It actually turns out that the lowest-energy state of each Heisenberg trimer is two-fold degenerate if all three surrounding Ising spins are aligned alike (all three Ising spins point either 'up' or 'down'), while there is just one lowest-energy state from the ground-state manifold provided that two from three Ising spins are aligned alike and the third spin points in the opposite direction (remember that the lowest-energy state of the trimeric unit is three-fold degenerate irrespective of a spin configuration of monomeric spins within the Ising model). With regard to this, the residual entropy of the disordered spin liquid phase is for the quantum Ising-Heisenberg model significantly lower than for its semi-classical Ising limit $S_0/N_T k_B = 0.2806$ and 0.4752 , respectively, which implies that quantum fluctuations partially lift a macroscopic degeneracy of the ground-state manifold. The most surprising finding stemming from our study is that the zero-point entropy of the spin-1/2 Ising-Heisenberg model is the same for arbitrary but non-zero anisotropy Δ and this observation suggests that the semi-classical Ising limit represents a very special limiting case of the model under consideration.

To provide an independent check of the aforementioned scenario, we depict in Fig. 3 temperature variations of the effective interaction $\beta J_{\text{kag}}^{\text{eff}}$ for several values of the ratio $J_H/|J_I|$ and two different values of the anisotropy constant $\Delta = 0$ and 1 , respectively. It should be mentioned that the particular case with $\Delta = 1$ qualitatively resembles temperature dependences of the mapping parameter $\beta J_{\text{kag}}^{\text{eff}}$ for the Ising-Heisenberg model with any $\Delta \neq 0$. The considered model system is spontaneously long-range ordered below certain critical temperature if and only if the effective interaction parameter $\beta J_{\text{kag}}^{\text{eff}}$ is greater than the critical value $\beta_c J_{\text{kag}} = \ln(3+2\sqrt{3})$ shown in Fig. 3 as a broken line. In agreement with the afore-described ground-state analysis, the effective interaction starts from zero, then gradually increases to some local maximum before it finally goes to zero by increasing temperature whenever $\Delta = 0$ and $J_H/|J_I| < -1$. On the other hand, the effective interaction generally starts from the value $\ln 2$, then exhibits a temperature-induced local maximum before it finally tends to zero whenever $\Delta \neq 0$ and $J_H/|J_I| < -2/(2+\Delta)$. It is also quite evident from Fig. 3 that the spin system remains disordered over the whole temperature range for any $J_H/|J_I| < -2/(2+\Delta)$, since the effective interaction $\beta J_{\text{kag}}^{\text{eff}}$ never crosses the critical value $\beta_c J_{\text{kag}}$ that is needed to invoke a spontaneous ordering. This observation would suggest that the Ising-Heisenberg model in question cannot exhibit a

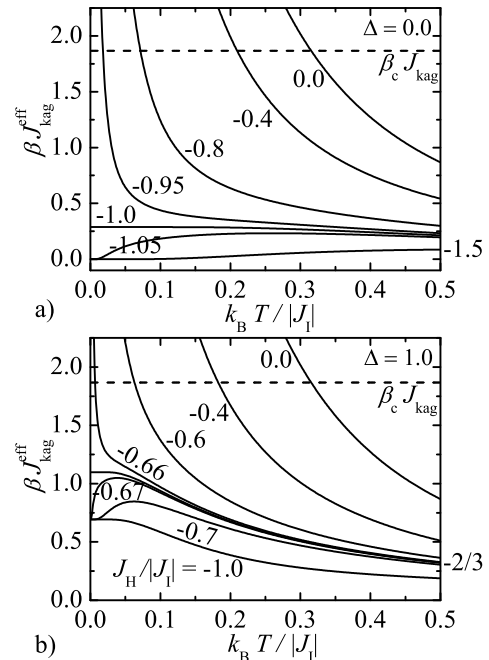


FIG. 3: Temperature dependences of the effective interaction $\beta J_{\text{kag}}^{\text{eff}}$ for several values of the ratio $J_H/|J_I|$ and two different anisotropy constants: (a) $\Delta = 0$; (b) $\Delta = 1$. Broken line shows the critical point $\beta_c J_{\text{kag}} = \ln(3 + 2\sqrt{3})$ of the corresponding spin-1/2 Ising model on the Kagomé lattice.

temperature-induced reentrant phase transition from the disordered towards the spontaneously ordered phase regardless of whether $\Delta = 0$ or $\Delta \neq 0$.

At this point, let us proceed to a discussion of the finite-temperature phase diagram. The critical temperature of the spin-1/2 Ising-Heisenberg model on the triangulated Kagomé lattice can easily be calculated from the critical condition $\beta_c J_{\text{kag}}^{\text{eff}} = \ln(3 + 2\sqrt{3})$, which ensures that the corresponding spin-1/2 Ising model on the Kagomé lattice is precisely at the critical point. Note that this critical condition is essentially equivalent to a graphical solution that finds points of intersection between the temperature dependence of the effective interaction $\beta J_{\text{kag}}^{\text{eff}}$ and the critical point $\beta_c J_{\text{kag}} = \ln(3 + 2\sqrt{3})$ of the spin-1/2 Ising model on the Kagomé lattice (see Fig. 3). The dependence of dimensionless critical temperature $k_B T_c/|J_I|$ on the ratio $J_H/|J_I|$ is displayed in Fig. 4 for several values of the anisotropy parameter Δ . As one can see, the critical temperature monotonically decreases by decreasing the ratio $J_H/|J_I|$ until it vanishes at the ground-state phase boundary (20) whenever the easy-axis exchange anisotropies $\Delta < 1$ are assumed. By contrast, the interesting non-monotonic dependence of the critical temperature may be observed for the easy-plane anisotropies $\Delta > 1$ presumably due to a competition between the easy-axis Ising interaction J_I and the easy-plane Heisenberg interaction $J_H(\Delta)$ before the critical line finally tends to zero-temperature limit consistent with the ground-state boundary (20). Several limiting

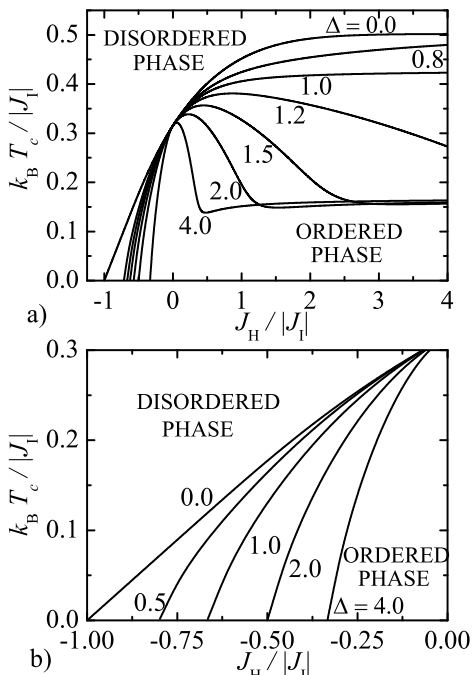


FIG. 4: The dimensionless critical temperature $k_B T_c / |J_I|$ as a function of the ratio $J_H / |J_I|$ for different values of the exchange anisotropy Δ . Fig. 4b shows a detail of the finite-temperature phase diagram, where the critical temperature tends towards the zero temperature.

cases of the model under investigation can be checked. First, the critical line of the spin-1/2 Ising model on the triangulated Kagomé lattice originally reported by Zheng and Sun²⁵ and later rederived by Loh, Yao, and Carlson,²⁶ is recovered on assumption that $\Delta = 0$. By assuming $J_H / |J_I| = 0$, on the other hand, all critical lines meet at a common critical point

$$\frac{k_B T_c}{|J_I|} = \frac{1}{2 \ln \left(\sqrt{3 + 2\sqrt{3}} + \sqrt{2 + 2\sqrt{3}} \right)} \doteq 0.3154, \quad (21)$$

which is consistent with the critical temperature of the spin-1/2 Ising model on the decorated Kagomé lattice. It is also quite interesting to check the asymptotic behavior of the critical temperature achieved in the limit $J_H / |J_I| \rightarrow \infty$ that corresponds to the infinitely strong ferromagnetic Heisenberg interaction. If $\Delta < 1$, the critical temperature asymptotically reaches the value

$$\frac{k_B T_c}{|J_I|} = \frac{1}{\ln \left(2 + \sqrt{3} + \sqrt{6 + 4\sqrt{3}} \right)} \doteq 0.5021, \quad (22)$$

while for $\Delta > 1$ it strikingly decreases down to one third of this asymptotic value

$$\frac{k_B T_c}{|J_I|} = \frac{1}{3 \ln \left(2 + \sqrt{3} + \sqrt{6 + 4\sqrt{3}} \right)} \doteq 0.1673. \quad (23)$$

For the particular case $\Delta = 1$, the critical temperature of the spin-1/2 Ising-Heisenberg model on the triangulated

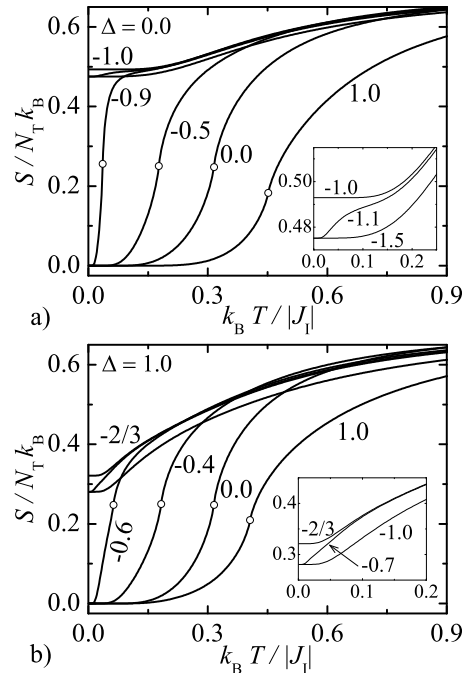


FIG. 5: Thermal variations of the entropy for different values of the ratio $J_H / |J_I|$, which are indicated by the numbers associated with each line, and two different values of the anisotropy constant: (a) $\Delta = 0$; (b) $\Delta = 1$. The insert shows the low-temperature behavior for special cases, where the entropy tends towards its residual values.

Kagomé lattice acquires in the limit $J_H / |J_I| \rightarrow \infty$ the asymptotic value $k_B T_c / |J_I| \doteq 0.4285$.

Next, let us turn our attention to temperature dependences of some thermodynamic quantities. Fig. 5 depicts temperature variations of the entropy calculated for several values of the ratio $J_H / |J_I|$ and two different values of the anisotropy $\Delta = 0$ and 1, respectively. As it can be clearly seen, the standard S-shaped dependence with a weak energy-type singularity located at critical points of the order-disorder phase transitions, which are schematically shown in Fig. 5 as open circles, gradually shifts towards zero temperature upon strengthening the antiferromagnetic Heisenberg interaction until the weak singularity completely disappears from the entropy dependence whenever $J_H / |J_I| < -2 / (2 + \Delta)$. Under this circumstance, the displayed thermal dependences tend asymptotically towards the zero-point entropy $S_0 / N_T k_B = 0.2806$ or 0.4752 depending on whether $\Delta \neq 0$ or $\Delta = 0$, respectively. The low-temperature behavior of the entropy, which is for better clarity shown in the insert of Fig. 5, thus provides an independent confirmation of the macroscopic degeneracy that appears within the disordered spin liquid ground states.

Finally, let us conclude our analysis of thermodynamics by exploring temperature dependences of the zero-field specific heat. For illustration, some typical thermal variations of the specific heat are plotted in Figs. 6 and 7 for several values of the ratio $J_H / |J_I|$ and two different val-

ues of the exchange anisotropy $\Delta = 0$ and 1, respectively. The upper panel in both figures depicts the particular cases with the spontaneously long-range ordered ground state, whereas the lower panel shows the particular cases with the disordered spin liquid ground state. In accordance with the above statement, all temperature dependences of the heat capacity shown in both upper panels display a logarithmic singularity from the standard Ising universality class, which is associated with the continuous (second-order) phase transition between the spontaneously ordered and disordered phases. Even although the specific heat curves displayed in Figs. 6 and 7 have several common features, there are nevertheless a few important differences. In both cases, the marked round maximum is superimposed on the high-temperature tail of the specific heat singularity by considering a strong ferromagnetic intra-trimer interaction $J_H/|J_I| \gg 1$ (see Figs. 6a and 7a). However, it can be also clearly seen that this round maximum is much more pronounced in the Ising model with $\Delta = 0$ than in the Ising-Heisenberg model with $\Delta = 1$. It is worthwhile to remark, moreover, that the round maximum in the high-temperature tail of the specific heat can be also observed when taking into account the antiferromagnetic intra-trimer interaction $J_H/|J_I| < 0$ (see Figs. 6bc and 7bc), but in this particular case, the robust hump develops only if the ratio $J_H/|J_I|$ is close enough to the boundary value (20). In this parameter space, the most important difference between the specific heat curves of the Ising and Ising-Heisenberg models lies in an appearance of the additional marked shoulder, which appears in the low-temperature tail of the heat capacity in the latter model only (Fig. 7c), whereas this feature is obviously missing in the relevant dependence of the former model (Fig. 6c).

Last but not least, let us comment on temperature dependences of the specific heat by considering some typical cases that correspond to a spin system with the disordered spin liquid ground state (the lower panels in Figs. 6 and 7). Apparently, the temperature dependence with a single maximum is obtained by selecting the ratio $J_H/|J_I|$ exactly from the ground-state boundary (20) between the spontaneously ordered and disordered phases (see Figs. 6d and 7d). Note that this maximum is nevertheless much less symmetric for the Ising-Heisenberg model (Figs. 7d) than for its Ising counterpart (Figs. 6d), while both models exhibit a quite similar uprising of the additional low-temperature shoulder upon a consecutive slight decrease of the ratio $J_H/|J_I|$. As evidenced by Fig. 7e, the specific heat of the Ising-Heisenberg model gradually loses its irregular shape upon further decrease of the interaction parameter $J_H/|J_I|$. It is noteworthy, moreover, that the specific heat curve with two marked rounded maxima appear by assuming a sufficiently strong antiferromagnetic intra-trimer interaction $J_H/|J_I| \ll -1$ (Figs. 6f and 7f), whereas the more negative is the ratio $J_H/|J_I|$, the more evident is the double-peak structure of the zero-field specific heat curve. However, it should be also pointed out that the temperature dependence

with the double-peak specific heat emerges in the Ising-Heisenberg model with $\Delta = 1$ for much smaller geometric frustration (i.e. less negative ratio $J_H/|J_I|$) than for the Ising model with $\Delta = 0$. Notwithstanding this observation, the specific heat curves with two well-separated maxima might be expected for the series of polymeric coordination compounds $\text{Cu}_9\text{X}_2(\text{cpa})_6$ for which a rough estimate of the ratio $|J_{aa}/J_{ab}| \approx 40$ has been made according to the experimentally measured susceptibility data.²³

IV. CONCLUDING REMARKS

The present article provides a survey of exact analytical results for the spin-1/2 Ising-Heisenberg model on the triangulated Kagomé (triangles-in-triangles) lattice, which has been proposed in order to shed light on a frustrated magnetism of the series of $\text{Cu}_9\text{X}_2(\text{cpa})_6$ polymeric coordination compounds. The model under investigation has exactly been solved with the help of generalized star-triangle transformation that establishes a precise mapping relationship to the corresponding spin-1/2 Ising model on the Kagomé lattice. Exact results for the ground-state and finite-temperature phase diagrams, as well as, several thermodynamic quantities such as the Helmholtz free energy, internal energy, entropy, and specific heat, have been derived and discussed in detail.

Even though a theoretical description based on the hybrid Ising-Heisenberg model may not be fully realistic for true magnetic materials from the family of copper-based coordination compounds (Heisenberg model would be of course more adequate), it is quite reasonable to expect that the presented exact results illustrate many important features of the series of three isostructural compounds $\text{Cu}_9\text{X}_2(\text{cpa})_6$. It is really plausible to argue that the suggested model correctly takes into account quantum effects closely connected with the stronger intra-trimer Heisenberg interaction J_H , whereas the Ising character of the weaker monomer-trimer interaction J_I might be regarded as at least rather reasonable first-order approximation. This approximation should be altogether acceptable especially in the highly frustrated region $J_H/|J_I| \ll -2/(2 + \Delta)$, where the 'Ising' spins located at the monomeric sites are completely free to flip without any energy cost owing to a strong geometric frustration produced by the trimeric 'Heisenberg' spins. From this perspective, it is quite tempting to conjecture that the zero-field specific heat of $\text{Cu}_9\text{X}_2(\text{cpa})_6$ compounds should exhibit a notable temperature dependence with two outstanding round maxima, which are well separated from each other because the antiferromagnetic intra-trimer interaction is roughly two orders of magnitude stronger than the ferromagnetic monomer-trimer interaction.

In agreement with our expectations, it also has been demonstrated that quantum fluctuations introduced through the non-zero exchange anisotropy Δ help to destroy spontaneous (ferromagnetic or ferrimagnetic)

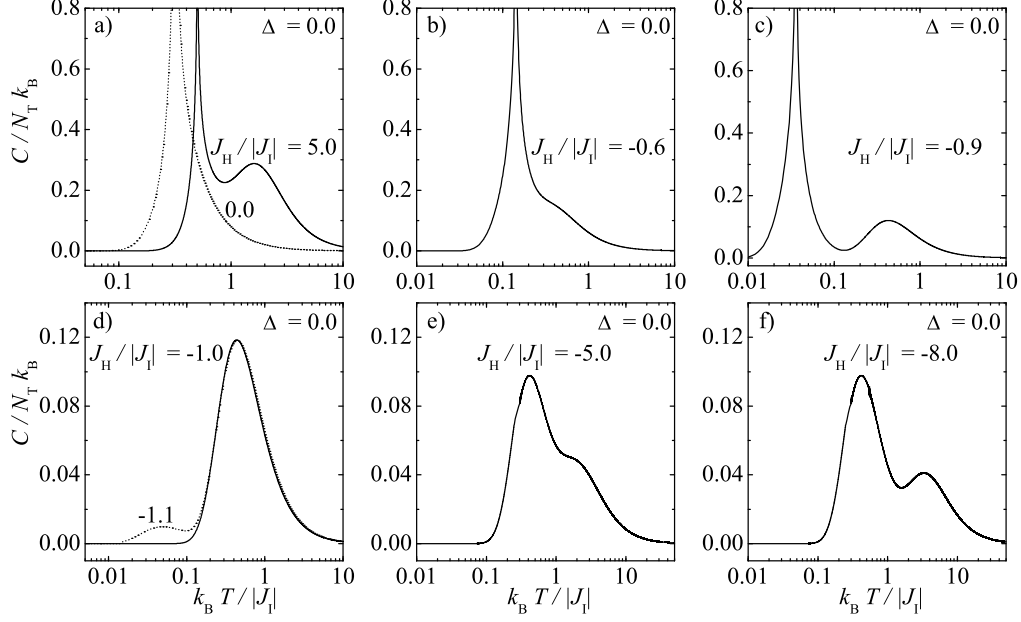


FIG. 6: Some typical temperature dependences of the zero-field specific heat of the spin-1/2 Ising model on the triangulated Kagomé lattice with $\Delta = 0$, which can be obtained by changing a strength of the interaction ratio $J_H/|J_I|$.

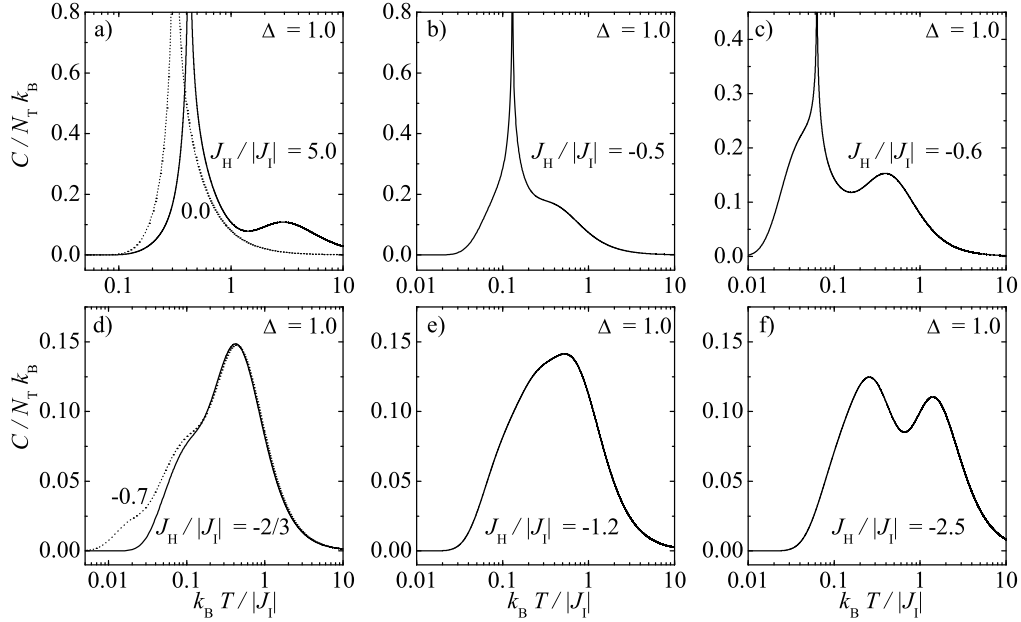


FIG. 7: Some typical temperature dependences of the zero-field specific heat of the spin-1/2 Ising-Heisenberg model on the triangulated Kagomé lattice with $\Delta = 1$, which can be obtained by changing a strength of the interaction ratio $J_H/|J_I|$.

long-range ordering. As a matter of fact, it can be readily understood from Eq. (20) that the increase in the anisotropy parameter Δ suppresses a strength of the antiferromagnetic intra-trimer interaction that is needed to prevent spontaneous ordering. However, the most surprising finding to emerge from the present study closely relates to a substantial decline of the residual entropy

of disordered spin liquid state, which appears on assumption that there is arbitrary but non-zero exchange anisotropy Δ . It actually turns out that the quantum fluctuations partially lift a rather high macroscopic degeneracy of the disordered spin liquid state and consequently, the zero-point entropy of the quantum Ising-Heisenberg model $S_0/N_T k_B = 0.2806$ is for any $\Delta \neq 0$

significantly lower than the zero-point entropy of the semi-classical Ising model $S_0/N_T k_B = 0.4752$ achieved in the limiting case $\Delta = 0$. From this point of view, another interesting question arises whether or not the residual entropy of the spin-1/2 Heisenberg model on the triangulated Kagomé lattice will be completely removed by the order-from-disorder mechanism³⁶ when accounting for the Heisenberg character of the monomer-trimer interaction as well. In order to clarify this unresolved issue, it is necessary to perform a rather extensive exact numerical diagonalization of the full Heisenberg Hamiltonian, or, alternatively, it would be also possible to use the exact solution of the Ising-Heisenberg model as a starting point of more general perturbative treatment.

Note added

Shortly after our manuscript has been submitted for publication, Yao *et al.*³⁷ has completed a similar work dealing with the spin-1/2 Ising-Heisenberg model on the triangulated Kagomé lattice. The main difference between our procedure and the one of Yao *et al.*³⁷ lies in the way of calculating the energy spectrum of Heisenberg trimer and its three enclosing Ising spins. In our procedure, we have firstly performed an exact diagonalization of the Heisenberg trimer in some generally non-uniform local field produced by three surrounding Ising spins and then, we have considered two symmetry-distinct configuration of the enclosing Ising spins in order to establish a precise mapping relationship with the corresponding

spin-1/2 Ising model. In the procedure developed by Yao *et al.*³⁷ the authors first consider two symmetry-distinct configurations of the enclosing Ising spins and then, they diagonalize the Heisenberg trimer for both symmetry-distinct configurations of the surrounding Ising spins. In a such way, they were able to avoid rather cumbersome expressions for the roots of cubic equations, which otherwise occur when diagonalizing the Heisenberg trimer in some generally non-uniform local magnetic field. Despite this difference, both procedures turn out to be completely equivalent as it could be easily checked from a comparison of the effective mapping parameter $\beta J_{\text{kag}}^{\text{eff}}$ calculated from our Eqs. (8-13) and Eqs. (7-8,13-14) of Yao *et al.*,³⁷ respectively. Exact results presented in both manuscripts for the ground-state and finite-temperature phase diagrams, Helmholtz free energy, internal energy and entropy are consequently in a very good accordance.

Acknowledgments

J. Strečka would like to thank Japan Society for the Promotion of Science for the award of postdoctoral fellowship (ID No. PE07031) under which part of this work was carried out. This work was supported by the Slovak Research and Development Agency under the contract LPP-0107-06. The financial support provided by Ministry of Education of Slovak Republic under the grant No. VEGA 1/0128/08 is also gratefully acknowledged.

* Electronic address: jozef.strecka@upjs.sk, jozkos@pobox.sk; URL: <http://158.197.33.91/~strecka>

¹ G. Misguich and C. Lhuillier, in *Frustrated Spin Systems*, edited by H.T. Diep (World Scientific, Singapore, 2004).

² J. Richter, J. Schulenburg, and A. Honecker, in *Quantum Magnetism*, edited by U. Schollwöck, J. Richter, D.J.J. Farnell, and R.F. Bishop (Springer, Berlin, 2004), Lecture Notes in Physics, Vol. 645.

³ A. Honecker, J. Schulenburg, and J. Richter, *J. Phys.: Condens. Matter* **16**, S749 (2004).

⁴ C. Lhuillier and G. Misguich, *Lecture Notes in Physics* **595**, 161 (2002); C. Lhuillier, *Frustrated Quantum Magnets*, cond-mat/0502464.

⁵ S. Miyashita, *J. Phys. Soc. Jpn.* **55**, 3605 (1986); H. Nishimori and S. Miyashita, *J. Phys. Soc. Jpn.* **55**, 4448 (1986); D.A. Huse and V. Elser, *Phys. Rev. Lett.* **60**, 2531 (1988); H. Nishimori and H. Nakanishi, *J. Phys. Soc. Jpn.* **57**, 626 (1988); A.V. Chubukov and D.I. Golosov, *J. Phys.: Condens. Matter* **3**, 69 (1991); B. Bernu, C. Lhuillier, and L. Pierre, *Phys. Rev. Lett.* **69**, 2590 (1992); P.W. Leung and K.J. Runge, *Phys. Rev. B* **47**, 5861 (1993); B. Bernu, P. Lecheminant, C. Lhuillier, and L. Pierre, *Phys. Scr.* **49**, 192 (1993); *Phys. Rev. B* **50**, 10048 (1994); L. Capriotti, A.E. Trumper, and S. Sorella, *Phys. Rev. Lett.* **82**, 3899 (1999); A. Honecker, *J. Phys.: Condens. Matter* **11**, 4697 (1999); C. Lhuillier, P. Sindzingre, and J.B. Fouet, *Can. J. Phys.* **79**, 1525 (2001);

⁶ V. Elser, *Phys. Rev. Lett.* **62**, 2405 (1989); C. Zeng and V. Elser, *Phys. Rev. B* **42**, 8436 (1990); S. Sachdev, *ibid.* **45**, 12377 (1992); J.T. Chalker and J.F.G. Eastmond, *ibid.* **46**, 14201 (1992); R.R.P. Singh and D.A. Huse, *Phys. Rev. Lett.* **68**, 1766 (1992); P.W. Leung and V. Elser, *Phys. Rev. B* **47**, 5459 (1993); N. Elstner and A.P. Young, *ibid.* **50**, 6871 (1994); C. Zeng and V. Elser, *ibid.* **51**, 8318 (1995); P. Lecheminant, B. Bernu, C. Lhuillier, L. Pierre, and P. Sindzingre, *ibid.* **56**, 2521 (1997); Ch. Waldtmann, H.-U. Everts, B. Bernu, C. Lhuillier, P. Sindzingre, P. Lecheminant, and L. Pierre, *Eur. Phys. J. B* **2**, 501 (1998); F. Mila, *Phys. Rev. Lett.* **81**, 2356 (1998); M. Mambrini and F. Mila, *Eur. J. Phys. B* **17**, 651 (2000); K. Hida, *J. Phys. Soc. Jpn.* **70**, 3673 (2001); D.C. Cabra, M.D. Grynberg, P.C.W. Holdsworth, and P. Pujol, *Phys. Rev. B* **65**, 094418 (2002); J. Schulenburg, A. Honecker, J. Schnack, J. Richter, and H.J. Schmidt, *Phys. Rev. Lett.* **88**, 167207 (2002); D.C. Cabra, M.D. Grynberg, P.C.W. Holdsworth, A. Honecker, P. Pujol, J. Richter, D. Schmalfuss, and J. Schulenburg, *Phys. Rev. B* **71**, 144420 (2005).

⁷ L.B. Marston and C. Zeng, *J. Appl. Phys.* **69**, 5962 (1991); A.V. Syromyatnikov and S.V. Maleyev, *Phys. Rev. B* **66**, 132408 (2002); P. Nikolić and T. Senthil, *ibid.* **68**, 214415 (2003); R. Budnik and A. Auerbach, *Phys. Rev. Lett.* **93**, 187205 (2004); R.R.P. Singh and D.A. Huse, *Phys. Rev. B* **76**, 180407(R) (2007).

⁸ B.S. Shastry and B. Sutherland, *Physica B&C* **108**, 1069

- (1981); Z. Weihong, C.J. Hamer, and J. Oitmaa, Phys. Rev. B **60**, 6608 (1999). S. Miyahara and K. Ueda, Phys. Rev. Lett. **82** 3701 (1999); E. Müller-Hartmann, R.R.P. Singh, C. Knetter, and G.S. Uhrig, *ibid.* **84**, 1808 (2000); A. Koga and N. Kawakami, *ibid.* **84**, 4461 (2000); C.H. Chung, J.B. Marston, and S. Sachdev, Phys. Rev. B **64**, 134407 (2001); Y. Takushima, A. Koga, and N. Kawakami, J. Phys. Soc. Jpn. **70**, 1369 (2001); A. Läuchli, S. Wessel, and M. Sigrist, Phys. Rev. B **66**, 014401 (2002); S. Miyahara and K. Ueda, J. Phys.: Condens. Matter **15**, R327 (2003).
- ⁹ J. Richter, J. Schulenburg, A. Honecker, and D. Schmalfuss, Phys. Rev. B **70**, 174454 (2004); G. Misguich and P. Sindzingre, J. Phys.: Condens. Matter **19**, 145202 (2007).
- ¹⁰ S. E. Palmer and J. T. Chalker, Phys. Rev. B **64**, 094412 (2001); W. Brenig and A. Honecker, *ibid.* **65**, 140407 (2002); B. Canals, *ibid.* **65**, 184408 (2002); J.B. Fouet, M. Mambrini, P. Sindzingre, and C. Lhuillier, *ibid.* **67**, 054411 (2003); J. Richter, J. Schulenburg, A. Honecker, J. Schnack, and H.-J. Schmidt, J. Phys.: Condens. Matter **16**, S779 (2004).
- ¹¹ R. Siddharthan and A. Georges, Phys. Rev. B **65**, 014417 (2001); P. Tomczak and J. Richter, J. Phys. A: Math. Gen. **36**, 5399 (2003); J. Richter, O. Derzhko, and J. Schulenburg, Phys. Rev. Lett. **93**, 107206 (2004); P. Tomczak, A. Molinska, J. Richter, and J. Schulenburg, Acta Phys. Pol. A **109**, 781 (2006); J. Richter, J. Schulenburg, P. Tomczak, and D. Schmalfuss, cond-mat/0411673.
- ¹² M. Troyer, H. Kontani, and K. Ueda, Phys. Rev. Lett. **76**, 3822 (1996); M. Troyer, M. Imada, and K. Ueda, J. Phys. Soc. Jpn. **66**, 2957 (1997); P. Tomczak, J. Schulenburg, J. Richter, and A.R. Ferchmin, J. Phys.: Condens. Matter **13**, 3851 (2001); A. Collins, J. McEvoy, D. Robinson, C.J. Hamer, and Z. Weihong, Phys. Rev. B **73**, 024407 (2006); Z. Weihong, J. Oitmaa, and C.J. Hamer, *ibid.* **75**, 184418 (2007).
- ¹³ T. Inami, Y. Ajiro, and T. Goto, J. Phys. Soc. Jpn. **65**, 2374 (1996).
- ¹⁴ H. Tanaka, T. Ono, H. Aruga Katori, H. Mitamura, F. Ishikawa, and T. Goto, Progr. Theor. Phys. Suppl. **145**, 101 (2002); T. Ono, H. Tanaka, H. Aruga Katori, F. Ishikawa, H. Mitamura, and T. Goto, Phys. Rev. B **67**, 104431 (2003); T. Ono, H. Tanaka, O. Kolomyiets, H. Mitamura, T. Goto, K. Nakajima, A. Oosawa, Y. Koike, K. Kakurai, J. Klenke, P. Smeibidle, and M. Meissner, J. Phys.: Condens. Matter **16**, S773 (2004); T. Ono, H. Tanaka, T. Nakagomi, O. Kolomyiets, H. Mitamura, F. Ishikawa, T. Goto, K. Nakajima, A. Oosawa, Y. Koike, K. Kakurai, J. Klenke, P. Smeibidle, M. Meissner, and H. Aruga Katori, J. Phys. Soc. Jpn. **74**, 135 (2005); T. Ono, H. Tanaka, O. Kolomyiets, H. Mitamura, F. Ishikawa, T. Goto, K. Nakajima, A. Oosawa, Y. Koike, K. Kakurai, J. Klenke, P. Smeibidle, M. Meissner, R. Coldea, A.D. Tennant, and J. Ollivier, Progr. Theor. Phys. Suppl. **159**, 217 (2005).
- ¹⁵ L.E. Svistov, A.I. Smirnov, L.A. Prozorova, O.A. Petrenko, L.N. Demianets, and A.Ya. Shapiro, Phys. Rev. B **67**, 094434 (2003); L.A. Prozorova, L.E. Svistov, A.I. Smirnov, O.A. Petrenko, L.N. Demianets, and A.Ya. Shapiro, J. Magn. Magn. Mater. **258-259**, 394 (2003); L.E. Svistov, A.I. Smirnov, L.A. Prozorova, O.A. Petrenko, A. Micheler, N. Büttgen, A.Ya. Shapiro, and L. N. Demianets, Phys. Rev. B **74**, 024412 (2006); A.I. Smirnov, H. Yashiro, S. Kimura, M. Hagiwara, Y. Narumi, K. Kindo, A. Kikkawa, K. Katsumata, A.Ya. Shapiro, and L.N. Demianets, *ibid.* **75**, 134412 (2007).
- ¹⁶ Y. Narumi, K. Katsumata, Z. Honda, J.-C. Domenge, P. Sindzingre, C. Lhuillier, Y. Shimaoka, T.C. Kobayashi, and K. Kindo, Europhys. Lett. **65**, 705 (2004); Y. Narumi, Z. Honda, K. Katsumata, J.-C. Domenge, P. Sindzingre, C. Lhuillier, A. Matsuo, K. Suga, and K. Kindo, J. Magn. Mater. **272-276**, 878 (2004).
- ¹⁷ H. Kageyama, K. Yoshimura, R. Stern, N.V. Mushnikov, K. Onizuka, M. Kato, K. Kosuge, C.P. Slichter, T. Goto, and Y. Ueda, Phys. Rev. Lett. **82**, 3168 (1999); K. Onizuka, H. Kageyama, Y. Narumi, K. Kindo, Y. Ueda, and T. Goto, J. Phys. Soc. Jpn. **69**, 1016 (2000); H. Kageyama, Y. Narumi, K. Kindo, K. Onizuka, Y. Ueda, and T. Goto, J. Alloy. Compd. **317-318**, 177 (2001); H. Kageyama, Y. Ueda, Y. Narumi, K. Kindo, M. Kosaka, and Y. Uwatoko, Prog. Theor. Phys. Suppl. **145**, (2002).
- ¹⁸ S. Michimura, A. Shigekawa, F. Iga, M. Sera, T. Takabatake, K. Ohoyama, and Y. Okabe, Physica B **378-380**, 596 (2006); S. Yoshii, T. Yamamoto, M. Hagiwara, A. Shigekawa, S. Michimura, F. Iga, T. Takabatake, and K. Kindo, J. Phys.: Conf. Ser. **51**, 59 (2006); F. Iga, A. Shigekawa, Y. Hasegawa, S. Michimura, T. Takabatake, S. Yoshii, T. Yamamoto, M. Hagiwara and K. Kindo, J. Magn. Mater. **310**, e443 (2007).
- ¹⁹ M.E. Zhitomirsky, Phys. Rev. B **67**, 104421 (2003); A. Honecker and J. Richter, Condens. Matter Phys. **8**, 813 (2005); O. Derzhko and J. Richter, Eur. Phys. J. B **52**, 23 (2006); A. Honecker and S. Wessel, Physica B **378-380**, 1098 (2006).
- ²⁰ J.E. Greedan, J. Mater. Chem. **11**, 37 (2001); A. Harrison, J. Phys.: Condens. Matter **16**, S553 (2004).
- ²¹ R.E. Norman, N.J. Rose, and R.E. Stenkamp, J. Chem. Soc.: Dalton Trans. (1987) 2905; R.E. Norman and R.E. Stenkamp, Acta Crystallogr. C **46**, 6 (1990); M. Gonzalez, F. Cervantes-Lee, and L.W. ter Haar, Mol. Cryst. Liq. Cryst. **233**, 317 (1993).
- ²² S. Maruti and L.W. ter Haar, J. Appl. Phys. **75**, 5949 (1994); S. Ateca, S. Maruti, and L.W. ter Haar, J. Magn. Mater. **147**, 398 (1995).
- ²³ M. Mekata, M. Abdulla, T. Asano, H. Kikuchi, T. Goto, T. Morishita, and H. Hori, J. Magn. Mater. **177-181** (1998) 731; M. Mekata, M. Abdulla, M. Kubota, and Y. Oohara, Can. J. Phys. **79**, 1409 (2001).
- ²⁴ A.P. Ramirez, Annu. Rev. Mater. Sci. **24**, 453 (1994); Handbook on Magnetic Materials **13**, 423 (2001)
- ²⁵ J. Zheng and G. Sun, Phys. Rev. B **71**, 052408 (2005).
- ²⁶ Y.L. Loh, D.X. Yao, and E.W. Carlson, Phys. Rev. B **77**, 134402 (2008).
- ²⁷ L. J. de Jongh and A. R. Miedema, *Experiments on Simple Magnetic Model Systems* (Taylor and Francis, London, 1974); Adv. Phys. **50**, 947 (2001); J. Yoon and E.I. Solomon, Coord. Chem. Rev. **251**, 379 (2007).
- ²⁸ S. Okubo, M. Hayashi, S. Kimura, H. Ohta, M. Motokawa, H. Kikuchi, H. Nagasawa, Physica B **246-247**, 553 (1998).
- ²⁹ R. Natori, Y. Watabe, and Y. Natsume, J. Phys. Soc. Jpn. **66**, 3687 (1997).
- ³⁰ J. Strečka, J. Magn. Mater. **316**, e346 (2007).
- ³¹ M.E. Fisher, Phys. Rev. **113**, 969 (1959).
- ³² I. Syozi, in *Phase Transitions and Critical Phenomena*, edited by C. Domb and M. S. Green (Academic Press, New York, 1972), Vol. 1.

- ³³ I. Syozi, *Progr. Theor. Phys.* **6**, 306 (1951).
- ³⁴ K. Kano and S. Naya, *Progr. Theor. Phys.* **10**, 158 (1953).
- ³⁵ C. Domb, *Adv. Phys.* **9**, 149 (1960).
- ³⁶ J. Villain, R. Bidaux, J.-P. Carton, and R. Conte, *J. Phys. (Paris)* **41**, 1263 (1980); E.F. Shender, *Sov. Phys. JETP* **56**, 178 (1982); J.N. Reimers and A.J. Berlinsky, *Phys. Rev. B* **48**, 9539 (1993); R. Moessner, S.L. Sondhi, and P. Chandra, *Phys. Rev. Lett.* **84**, 4457 (2000); R. Moessner and S.L. Sondhi, *Phys. Rev. B* **63**, 224401 (2001).
- ³⁷ D.X. Yao, Y.L. Loh, E.W. Carlson, and M. Ma, arXiv preprint: 0802.2719v1.
- ³⁸ To simplify further description, we will further refer to Cu^{2+} ions at the trimeric and monomeric sites as to the Heisenberg and Ising spins, respectively.